



Journal of applied research and technology

ISSN: 1665-6423

UNAM, Centro de Ciencias Aplicadas y Desarrollo Tecnológico

Pathak, Ashish

Effect of Cr on electronic and mechanical properties of TiS₂ compound: A first-principles study

Journal of applied research and technology, vol. 17, no. 4, 2019, pp. 302-312

UNAM, Centro de Ciencias Aplicadas y Desarrollo Tecnológico

DOI: <https://doi.org/10.22201/icat.16656423.2019.17.4.862>

Available in: <https://www.redalyc.org/articulo.oa?id=47471678007>

- How to cite
- Complete issue
- More information about this article
- Journal's webpage in redalyc.org

UNAM
redalyc.org

Scientific Information System Redalyc

Network of Scientific Journals from Latin America and the Caribbean, Spain and Portugal

Project academic non-profit, developed under the open access initiative



Original

Effect of Cr on electronic and mechanical properties of TiS_2 compound: A first-principles study

Ashish Pathak

Defence Metallurgical Research Laboratory, Kanchanbagh P.O., Hyderabad – 500058

Abstract: The electronic structural and mechanical properties for hexagonal structure of unpolarized TiS_2 , TiS_2Cr and spin-polarized TiS_2Cr compounds have been studied using first principles pseudo potential plane wave method. The equilibrium lattice constant values of unpolarized TiS_2 and TiS_2Cr compounds are in agreement with the available theoretical data. The unpolarized TiS_2 and TiS_2Cr compounds display metallic bonding whereas spin-polarized TiS_2Cr shows directional bonding. Based on shear to bulk modulus (G/B) ratios, the unpolarized TiS_2 and TiS_2Cr compounds are associated with ductile behaviour whereas spin-polarized TiS_2Cr compound shows brittle nature. The Debye temperature (θ_D) is higher for spin-polarized TiS_2Cr .

Keywords: Chalcogenides; First-principles; Crystal structure; Electronic structural; Mechanical properties

1. INTRODUCTION

Titanium sulphide is a semi-metallic in its ground state. Yan-Bin et al. (Yan-Bin et al, 2007) reported the metallic behaviour in the self-intercalated TiS_2 where the coulomb interaction with metal Ti-atom decreases the overlapping of orbitals. The $\text{Ti}(3d)\text{-S}(3p)$ hybridization is responsible for the covalent bonding in TiS_2 . Transition metal chalcogenides show interesting behaviour due to their layered and two dimensional symmetric structures. The metallic species can be easily intercalated into the pure material which is possible due to weak interlayer van der Waals attraction (vdW). Strong hybridization occurs

among $\text{M}(3d)$, $\text{Ti}(3d)$ and $\text{S}(3p)$ with intercalation with transition metals (M). These chalcogenides have been useful in forming a family of intercalated compounds (Bardhan, Kirczenow & Irwin, 1985; Tonti, Pettenkofer & Jaegermann, 2004; Whittingham, 1987). TiS_2 has been utilised for oxygen catalyst for fuel cells (Baresel, Sarholz, Scharner, Schmitz & Bunsen Ges, 1974) whereas Li-TiS_2 has been explored as a future material for high energy batteries (Abraham & Alamgir, 1991). These observations have been supported by angle resolved inverse photoemission spectroscopy (ARIPES), angle resolved resonant photoemission spectroscopy (ARPES), X-ray photoemission spectroscopy (XPS) and high field magnetization measurements (Matsushita, Suga, Kimuta, Negishi, & Inoue, 1999; Ueda et al., 1986).

The bonding behaviour in intercalated TiS_2 has been studied theoretically (Cui et al., 2006; Kim, Li, Tanaka,

* Corresponding author.

E-mail address: ashishpathak@dmrl.drdo.in (Ashish Pathak).

Peer Review under the responsibility of Universidad Nacional Autónoma de México.

Koyama & Adachi, 2000; Suzuki, Yamasaki & Motizuki, 1988; Yamasaki, Suzuki & Motizuki, 1987). It has been pointed out that the transport properties of MTiS_2 are unusual and are dependent on those of the guest atom (Inoue, Moneta, Neigh & Sasaki, 1986; Inoue, Sadahiro & Negishi, 1991; Negishi, Yamada, Yuri & Inoue, 1997; Tazuke et al., 1988; Takase et al., 2000).

Recently, Sharma, Shukla, Dwivedi and Sharma (2015), have studied the electronic and transport properties of MTiS_2 ($M = \text{Cr, Mn and Fe}$). However, they have not addressed the mechanical properties of these compounds. In the present work the electronic, structural and mechanical properties of unpolarised TiS_2 , TiS_2Cr and spin-polarised TiS_2Cr have been investigated in the framework of density functional theory (DFT).

2. METHODOLOGY

All the calculations have been performed by *Abinit* software based on norm conserving pseudopotential method within density functional theory (DFT) (Gonze et al., 2002; 2005; 2009; Hohenberg & Kohn, 1964; Kohn & Sham, 1965; <http://www.abinit.org>). The generalized gradient approximation (GGA) using Perdew Burke Ernzerhof (PBE) formulation (Perdew, Burke & Ernzerhof, 1996) has been utilized to include exchange-correlation effects. The wave functions from real to reciprocal lattice have been converted using fast fourier transform algorithm (Goedecker, 1997). The wave functions have been determined self-consistently using conjugate gradient algorithm approach (Gonze, 1996; Payne, Teter, Allan, Arias, & Joannopoulos 1992). The Monkhorst-Pack scheme has been used for the integration over the Brillouin zone (BZ) (Monkhorst & Pack, 1976). The convergence with respect to plane wave cut-off energy and k-points has been checked. Accordingly, a plane wave cut-off energy of 80 Ry and k-mesh of $8 \times 8 \times 8$ have been used. The lattice constants have been relaxed to get the minimum energy. In order to get convergence, system is relaxed until the differences between energies or forces in two consecutive steps are less than 27×10^{-6} meV and 2.6 meV/Å, respectively.

Abinit software has been utilized to calculate the elastic constants using the linear-response method. The linear response method is based on second order derivative of the total energy with respect to the strain. For the visualization of the crystal structure and 2D charge density, Xcrysden (Kokalj, 1999) software has been used.

3. RESULTS AND DISCUSSION

TiS_2 has a CdI_2 type hexagonal crystal structure with space group $P\bar{3}m1$ (164). The Wyckoff positions for Ti is $1a$ (0, 0, 0); the two S atoms are placed at $2d$ ($1/3, 2/3, 1/4$) and ($2/3, 1/3, 3/4$). TiS_2 exhibits strong covalent bonding between Ti and S atoms and weak Van der Waals attraction between the layers. The crystal structures of TiS_2 and TiS_2Cr compounds are shown in Fig. 1. Due to weak attractive vdW contacts between the slabs, TiS_2 can be easily cleaved along planes and hence can be easily intercalated by guest species. The guest Cr atom occupies the $1b$ (0, 0, 0.5) position, the structure of Cr intercalated in TiS_2 is shown in Fig. 1(b).

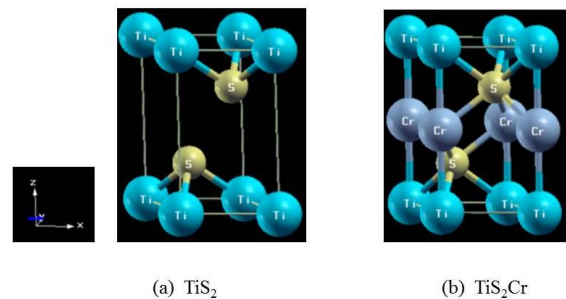


Fig. 1. Crystal structures of TiS_2 and TiS_2Cr compounds.

The lattice constants 'a' and 'c' of unpolarized TiS_2 , TiS_2Cr and spin-polarized TiS_2Cr compounds have been computed and given in Table 1. The equilibrium lattice constant has been achieved by changing lattice constant and computing the energy equivalent to each lattice constant. The lattice constant corresponding to lowest energy is considered as an equilibrium lattice constant. The lattice constant values obtained in present study for unpolarized TiS_2 and TiS_2Cr are in agreement with available theoretical values (Fang, De Groot & Hass, 1997; Yamasaki et al., 1987). However, the slight variation in the lattice constant values between present results and previous values are attributed due to the differences in the calculation schemes.

Density of states (DOS) and projected density of states (PDOS) of the unpolarized TiS_2 , TiS_2Cr and spin-polarized TiS_2Cr compounds are given in Figs. 2–4. The DOS for TiS_2 has a minimum at Fermi level (E_F) compared to a high peak in both unpolarized and spin polarised TiS_2Cr .

Table 1. The equilibrium lattice constants, calculated single crystal elastic constants for unpolarized TiS₂, TiS₂Cr and spin-polarized TiS₂Cr compounds. The other available theoretical values for lattice constants are also given for comparison (Yamasaki, Suzuki & Motizuki, 1987; Fang, de Groot & Hass, 1997).

| System | Magnetic-effect | a (Å) | c (Å) | C ₁₁ (GPa) | C ₁₂ (GPa) | C ₁₃ (GPa) | C ₃₃ (GPa) | C ₄₄ (GPa) |
|---------------------|-----------------|----------------------|----------------------|--------------------------|--------------------------|--------------------------|--------------------------|--------------------------|
| TiS ₂ | unpolarized | 3.5052 | 5.8591 | 98 | 35 | 51 | 79 | 48 |
| | | 3.407 ^{a,b} | 5.695 ^{a,b} | | | | | |
| TiS ₂ Cr | unpolarized | 3.5299 | 5.9004 | 150 | 58 | 94 | 185 | 76 |
| | | 3.418 ^a | 5.925 ^a | | | | | |
| | spin-polarized | 3.5303 | 5.9011 | 203 | 54 | 107 | 259 | 134 |

^aYamasaki et al., 1987

^bFang et al., 1997

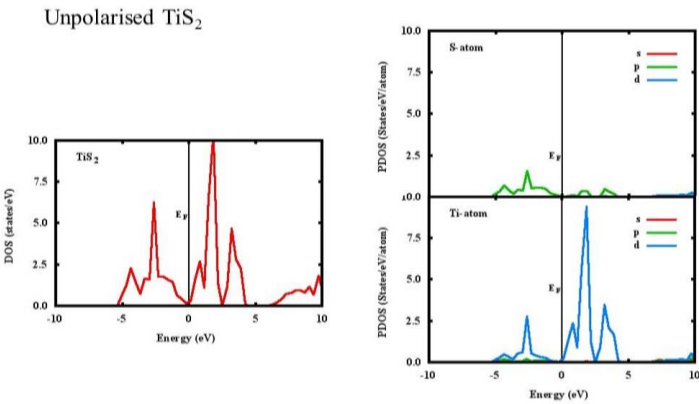


Fig. 2. Total DOS of the unpolarized TiS₂. The DOS of individual atoms are also shown.

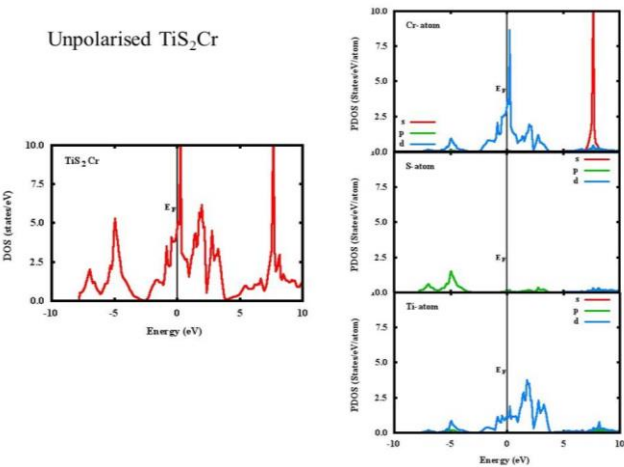


Fig. 3. Total DOS of the unpolarized TiS₂Cr. The DOS of individual atoms are also shown.

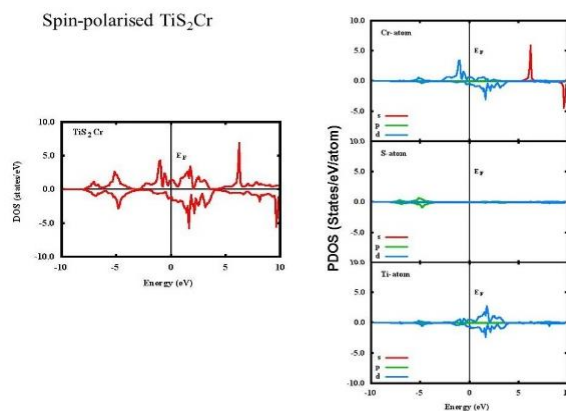


Fig. 4. Total DOS of the spin-polarized TiS_2Cr .
The DOS of individual atoms are also shown.

The DOS for the TiS_2 (Fig. 2) can be divided in three energy regions from -5 to 0, 0 to 5 and 5 to 10 eV. In the low energy region, there are two major peaks around -4.5 and -2.7 eV because of p and d orbital contribution of S and Ti atoms, respectively. In the 0-5 eV region, three peaks are found around 0.7, 1.8 and 3.3 eV mainly because of S(p) and Ti(d) orbital contributions whereas in high energy region (5–10 eV), a continuous energy band are seen. Similar behaviour of the DOS and peaks at similar positions are found in other published reports (Fang, Groot & Hass, 1997; Reshak, Kityk & Auluck, 2008; Sharma et al., 1999; Sharma et al., 2015). For unpolarised TiS_2Cr , the DOS can be divided in three energy regions namely, -7.5 to -2.5, -2.5 to 4 and 4 to 10 eV (Fig. 3). In the low energy region, two peaks are found around -7.0 and -5.0 eV. The peak at -5 eV is because of Cr(d), Ti(d) and S(p) orbital contributions. A continuous band found close to Fermi level having peaks at 0.2, 2.0 and 2.8 eV mainly because of Cr(d) and Ti(d) orbital contributions. In high energy region, again a continuous band with a high peak at 7.6 eV is found mainly because of Cr(s) orbital contribution.

Additionally, DOS for the spin-polarised TiS_2Cr in spin up and spin down has been shown in Fig. 4. The DOS for spin up can be divided in three energy regions namely, -8.0 to -2.8, -2.8 to 4 and 4 to 10 eV. For low energy region, two peaks are found at -7.1 and 5.2 eV mainly due to Cr(d), Ti(d) and S(p) orbital contribution, whereas continuous band having peaks at -1.0, 1.8 and 2.5 eV are

found close to Fermi level mainly because of Cr(d) and Ti(d) orbital contributions. In high energy region, a continuous band with one major peak at 6.2 eV is found mainly because of Cr(s) orbital contribution. Slightly shifted peaks are found in down spin. Further, the nature and location of peaks found in the present study are in good agreement with the reported peaks by Sharma et al. (2015). Two peaks (at 6.2 eV in up spin and 9.6 eV in down spin) which are originated due to s-orbital contribution of Cr-atom are not found in Sharma et al. (Sharma et al., 2015). Also, the PDOS shows strong Ti(d)-S(p) bonding for TiS_2 whereas strong Cr(d)-S(p), Cr(d)-Ti(d) and Ti(d)-S(s) bonding in unpolarised and spin-polarised TiS_2Cr (Figs. 2–4).

Further, the electronic band structures of unpolarised TiS_2 , unpolarised TiS_2Cr and spin-polarised TiS_2Cr have been shown in Figs. 5–7. These band structures are plotted in the high symmetry Γ -M-K- Γ -A directions in the irreducible brillouin zone (IBZ). It is to be noted that Fermi level (E_F) is set to 0 eV.

For TiS_2 , the band structure can be divided into two energy regions namely, -5 to 0 eV and 0 to 5 eV. These two regions are also called as bonding (-5 – 0 eV) and antibonding regions (0 – 5 eV). In the lower energy region, the energy states are because of p and d orbital contribution of S and Ti atoms, respectively. In conduction band region (0 to 5 eV) the energy states are mainly due to S(p) and Ti(d) orbital contributions. The valence band maximum (VBM) and the conduction band

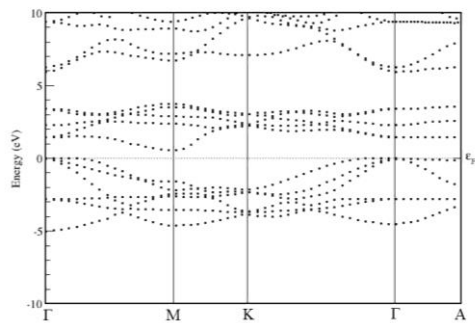


Fig. 5. Energy band structure for unpolarized TiS_2 along Γ -M-K- Γ -A directions.

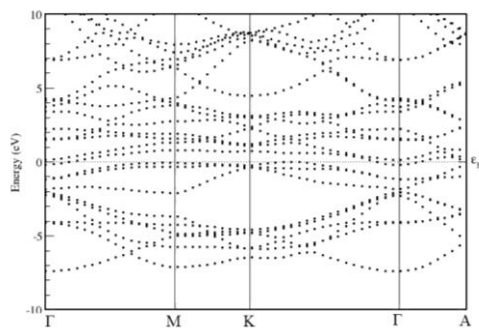


Fig. 6. Energy band structure for unpolarized TiS_2Cr along Γ -M-K- Γ -A directions.

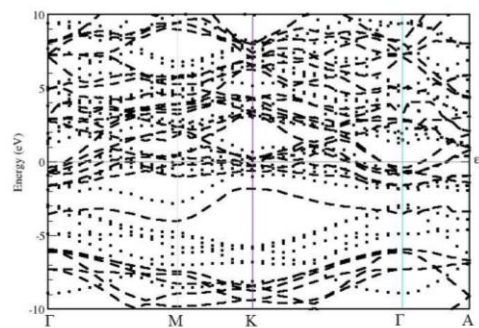


Fig. 7. Energy band structure for spin-polarized TiS_2Cr along Γ -M-K- Γ -A directions. Spin up and spin down band structures are shown with dotted and break lines, respectively.

minimum (CBM) are found at Γ and M symmetry points, respectively. Similar behaviour of band structure for TiS_2 has been found in other published reported (Fang, et al., 1997; Reshak et al., 2008; Sharma, Naut, 1999; Sharma et al., 2015).

For unpolarised TiS_2Cr , the band structure is divided into three energy regions. These are -7.5 to 0 eV, 0 to 5eV and 5 to 10 eV. In lower region, energy sates are of similar

nature of parent TiS_2 . However, the energy states are shifted towards lower energy side. These states are because of Cr(d), Ti(d) and S(p) orbital contribution. In the vicinity of E_F , near VBM and CBM additional states compared to TiS_2 are found mainly because of d-orbital contribution of Cr atom. In high energy region, apart from original states seen in TiS_2 few other states are also found due to Cr atom.

Further, for the spin-polarised TiS_2Cr , the spin up and spin down band structures are shown in Fig. 7. The band structure can be divided in three energy regions namely, -10 to -5 eV, -5 to 5 eV and 5 to 10 eV, respectively. In the lower region, slightly shifted and similar to TiS_2 energy states are found mainly because of Ti(d) and S(p) orbital contribution. Near E_F , a dense states due to mixing of different atomic states mainly due to d-orbital contribution of Cr and Ti atoms. In high energy region, a part from original states in TiS_2 few new states because of Cr atom are found. Finally, due to intercalation of Cr atom, the band structure modifies significantly and there is enhancement in the number of energy states in valence and conduction regions.

The corresponding 2D charge density distributions of the unpolarized TiS_2 , TiS_2Cr and spin-polarized TiS_2Cr compounds are shown in Figs. 8–10. TiS_2 displays strong and weak electronic interactions for Ti-S and S-S bonds respectively. TiS_2Cr shows strong electronic interactions for Cr-S compared to Ti-S and S-S bonds. The spin-polarization density or magnetization charge density (spin up minus spin down density) for spin-polarized TiS_2Cr compound (Fig. 10) shows that net magnetization for S atom is nearly zero whereas finite magnetization for Cr and Ti atoms. The extent of magnetization in Cr atoms is higher compared to Ti atoms. This is also supported by the calculated magnetic moment values for spin-polarized TiS_2Cr . The magnetic moments for Ti (m_{Ti}), Cr (m_{Cr}) and (m_{S}) are $-0.039 \mu_B$, $2.393 \mu_B$ and $-0.007 \mu_B$, respectively. The atomic magnetic moment for Ti (m_{Ti}) is anti-parallel to the Cr atom, indicating that spin-polarized TiS_2Cr compound is ferromagnetic.

The single crystal elastic properties of hexagonal structure are defined by five independent elastic constants namely, C_{11} , C_{12} , C_{33} , C_{13} and C_{44} and are given in Table 1. The nature of atomic bonding for hexagonal structures can be predicted based on Cauchy pressures (Pettifor & Aoki, 1991). These are well-defined as

$$C_1: C_{13} - C_{44} < 0, C_2: C_{12} - C_{66} < 0 \quad (1)$$

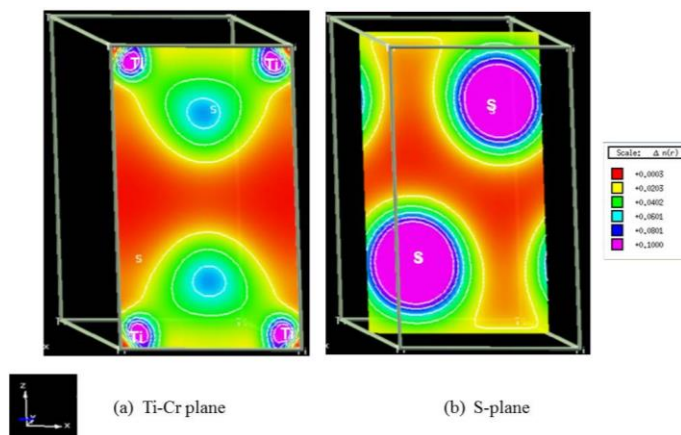


Fig. 8. 2D charge density distribution for the unpolarized TiS_2 compound in X-Z plane. Plane directions and charge density scales, units are also shown.

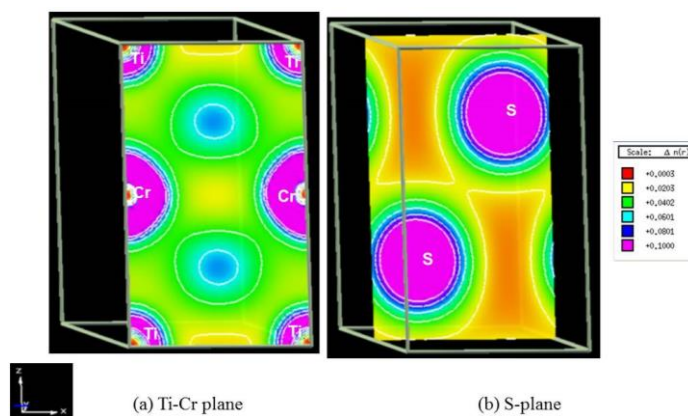


Fig. 9. 2D charge density distribution for the unpolarized TiS_2Cr compound in X-Z plane. Plane directions and charge density scales, units are also shown.

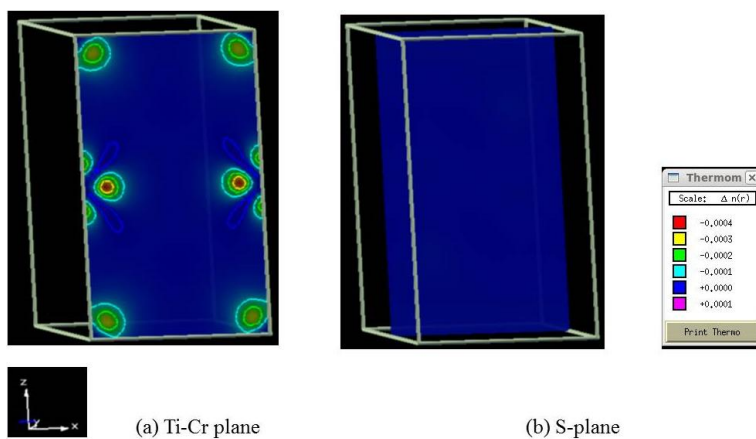


Fig. 10. 2D spin polarization density (spin up minus spin down charge density) for the spin-polarized TiS_2Cr compound in X-Z plane. Plane directions and charge density scales, units are also shown.

The negative Cauchy pressure shows directional bonding whereas positive value displays predominant metallic bonding. The computed values of Cauchy pressures of unpolarized TiS₂ and TiS₂Cr compounds are positive (Table 2) compared to negative values for spin-polarized TiS₂Cr. This clearly points towards the presence of major metallic bonds in unpolarized TiS₂ and TiS₂Cr whereas directional bonding in spin-polarized TiS₂Cr.

The values of elastic constants can also be utilized to predict the mechanical stability of these compounds. The Born stability criteria for hexagonal crystals are given in equations (2) and (3) respectively (Born, 1940; Fedorov, 1968).

$$S_1: C_{12} > 0, S_2: C_{33} > 0, S_3: C_{44} > 0, \tag{2}$$

$$S_4: (C_{11} - C_{12})/2 > 0$$

$$\text{and } S_5: (C_{11} + C_{12}) C_{33} - 2C_{13}^2 > 0 \tag{3}$$

The values for Born stability criteria suggest that these compounds (unpolarized TiS₂, TiS₂Cr and spin-polarized TiS₂Cr) are mechanically stable (Table 2). The anisotropy aspects (A) for hexagonal structure are defined below.

$$A_1 = \frac{2C_{44}}{(C_{11} - C_{12})}, A_2 = \frac{C_{33}}{C_{11}}, A_3 = \frac{C_{12}}{C_{13}} \tag{4}$$

The values of anisotropic factors should be unity for an isotropic crystal whereas away from unity point towards the presence of anisotropy. The anisotropic values (A₁, A₂, A₃) obtained in present study for unpolarized TiS₂, TiS₂Cr are (1.52, 0.81, 0.69), (1.65, 1.23, 0.62) respectively whereas for spin-polarized TiS₂Cr is (1.80, 1.28, 0.51). These values of anisotropic factors are away from unity indicating the presence of anisotropy in these materials.

Further, in the present study, these anisotropy values are also related to atomic bonding between different layered atoms. For TiS₂ system, z axis atomic positions are Ti (z= 0.0 Å), S1 (z = 1.4648 Å) and S2 (z = 4.3943 Å), respectively. The three Ti–S1 bond lengths are 2.4982 Å and forth one is 4.3043 Å. The S1–S2 bond length is 3.5606 Å. For unpolarised TiS₂Cr, z axis atomic positions are Ti (z = 0.0 Å), S1 (z = 1.4751 Å), Cr (z = 2.9502 Å) and S2 (z = 4.4253 Å), respectively. The three Ti–S1, three Cr–S1 and the three Cr–S2 bond lengths are equal (2.5158 Å). The forth bond for Ti–S1, Cr–S1 and Cr–S2 are also same (4.3347 Å).

Table 2. Calculated Cauchy pressures (C1, C2), Born stability criteria (S1, S2, S3, S4 and S5) and anisotropic values (A1, A2 and A3) for unpolarized TiS₂, TiS₂Cr and spin-polarized TiS₂Cr compounds.

| System | Magnetic-effect | C ₁ | C ₂ | S ₁ | S ₂ | S ₃ | S ₄ | S ₅ | A ₁ | A ₂ | A ₃ |
|---------------------|-----------------|----------------|----------------|----------------|----------------|----------------|----------------|----------------|----------------|----------------|----------------|
| | | (GPa) | | | | (GPa) | | | | | |
| TiS ₂ | unpolarized | 3 | 3.5 | 35 | 79 | 48 | 31.5 | 5305 | 1.52 | 0.81 | 0.69 |
| TiS ₂ Cr | unpolarized | 18 | 12 | 58 | 185 | 76 | 46 | 20808 | 1.65 | 1.23 | 0.62 |
| TiS ₂ Cr | Spin-polarised | -27 | -20.5 | 54 | 259 | 134 | 74.5 | 60731 | 1.80 | 1.28 | 0.51 |

Finally, for spin-polarised TiS_2Cr , z axis atomic positions are Ti ($z = 0.0 \text{ \AA}$), S1 ($z = 1.4753 \text{ \AA}$), Cr ($z = 2.9506 \text{ \AA}$) and S2 ($z = 4.4258 \text{ \AA}$), respectively. The neighbouring bonds for Ti-S1, Cr-S1 and Cr-S2 are of equal magnitude (2.5160 \AA). One bond for Ti-S1, Cr-S1 and Cr-S2 are of magnitude (4.3351 \AA). Therefore, the magnitude of atomic bonding between Ti-S1, Cr-S1 and Cr-S2 is same after the intercalation of Cr atom in the TiS_2 system. Further, the elastic anisotropic values such as A1 and A2 increase after the intercalation of Cr atom in the TiS_2 system (Table 2). This indicates that the atomic bonds along z-direction and shear plane perpendicular to z-direction are stiffer after intercalation of Cr atom in the TiS_2 system.

For polycrystalline hexagonal materials, Voigt (1928) and Reuss (1929) approximations can be utilized to estimate the upper and lower limit of elastic modulus. These are

$$B_V = [2(C_{11} + C_{12}) + C_{33} + 4C_{13}]/9 \quad (5)$$

$$G_V = [C_{11} + C_{33} - 2C_{13} + 6C_{44} + 5C_{66}]/15 \quad (6)$$

$$B_R = \frac{(C_{11} + C_{12})C_{33} - 2C_{13}^2}{C_{11} + C_{12} + 2C_{33} - 4C_{13}} \quad (7)$$

$$G_R = 15 / (8S_{11} + 4S_{33} - 4S_{12} - 8S_{13} + 6S_{44} + 3S_{66}) \quad (8)$$

$$S_{11} + S_{12} = C_{33}/C \quad (9)$$

$$S_{11} - S_{12} = 1/(C_{11} - C_{12}) \quad (10)$$

$$S_{13} = -C_{13}/C \quad (11)$$

$$S_{33} = (C_{11} + C_{12})/C \quad (12)$$

$$S_{44} = 1/C_{44} \quad (13)$$

$$S_{66} = 1/C_{66} \quad (14)$$

$$C = (C_{11} + C_{12})C_{33} - 2C_{13}^2 \quad (15)$$

Where B is bulk modulus while G_V and G_R are shear modulus values obtained by Voigt and Reuss approximations respectively.

The average value of these two estimates mentioned above is given by Hill (1952) approximation for hexagonal materials. The Voigt-Reuss-Hill (VRH) average values are given by

$$B = B_H = \frac{B_V + B_R}{2} \quad (16)$$

$$G = G_H = \frac{G_V + G_R}{2} \quad (17)$$

$$E = \frac{9BG}{3B + G} \quad (18)$$

$$\nu = \frac{3B - 2G}{2(3B + G)} \quad (19)$$

Where B ($=B_H$), G ($=G_H$), E and ν are bulk modulus, shear modulus, Young's modulus and Poisson's ratio, respectively.

The bulk modulus, shear modulus and Young's modulus (Table 3) exhibit maximum value for spin-polarized TiS_2Cr followed by unpolarized TiS_2Cr and TiS_2 . The values of shear and bulk modulus can also be utilized for The brittle and ductile behaviour of materials can also be predicted by taking ratios of G and B (Pugh, 1954). If the ratio (G/B) greater than 0.57, material is brittle otherwise related with ductile behaviour. Based on the G/B ratio, the spin-polarized TiS_2Cr is brittle whereas unpolarized TiS_2Cr and TiS_2 are ductile.

Debye temperature (θ_D) is one of the most significant parameter and it decides the thermal characteristics of the materials. The Debye temperature (θ_D) can be obtained from the mean sound velocity and can be calculated from the certain relations (Anderson, 1963; Sun, Ahuja & Schneider, 2004).

$$v_L = \sqrt{\frac{(B + \frac{4}{3}G)}{\rho}} \quad (20)$$

$$v_T = \sqrt{\frac{G}{\rho}} \quad (21)$$

$$v_m = \left[\frac{1}{3} \left(\frac{2}{v_T^3} + \frac{1}{v_L^3} \right) \right]^{-\frac{1}{3}} \quad (22)$$

Table 3. Calculated polycrystalline mechanical properties such as Bulk modulus (B), Shear Modulus (G), Young's modulus (E), G/B ratio and Poisson's ratio (ν) for unpolarized TiS₂, TiS₂Cr and spin-polarized TiS₂Cr compounds.

| System | Magnetic-effect | B (GPa) | G _V (GPa) | G _R (GPa) | G (GPa) | E (GPa) | G/B | ν |
|---------------------|-----------------|------------|-------------------------|-------------------------|------------|------------|-------|-------|
| TiS ₂ | unpolarized | 61 | 35 | 29 | 32 | 81 | 0.525 | 0.28 |
| | unpolarized | 106 | 55 | 53 | 54 | 139 | 0.509 | 0.28 |
| TiS ₂ Cr | spin-polarized | 130 | 91 | 86 | 89 | 217 | 0.685 | 0.22 |

Table 4. Calculated unit cell volume, density (ρ), longitudinal sound velocity (v_L), transverse sound velocity (v_T), mean sound velocity (v_m) and Debye temperature (θ_D) for unpolarised TiS₂, TiS₂Cr and spin-polarised TiS₂Cr compounds.

| Alloy | Magnetic-effect | Volume (Å ³) | ρ (gm/cm ³) | v_L (km/sec) | v_T (km/sec) | v_m (km/sec) | θ_D (K) |
|---------------------|-----------------|-----------------------------|---------------------------------|-------------------|-------------------|-------------------|-------------------|
| TiS ₂ | unpolarised | 62.3411 | 2.9806 | 5.8974 | 3.2766 | 3.6493 | 395 |
| TiS ₂ Cr | unpolarised | 63.6684 | 4.2744 | 6.4531 | 3.5543 | 3.9613 | 469 |
| | spin-polarised | 63.6847 | 4.2733 | 7.6282 | 4.5636 | 5.0499 | 598 |

where v_L , v_T and v_m are the longitudinal, transverse and mean sound velocities obtained using the shear modulus (G), bulk modulus (B) and the density (ρ).

The Debye temperature (θ_D) can be given as

$$\theta_D = \frac{h}{k} \left[\frac{3n}{4\pi} \left(\frac{N_A \rho}{M} \right) \right]^{\frac{1}{3}} v_m \quad (23)$$

where h is the Planck's constant, k is the Boltzmann's constant, N_A is the Avogadro's number, ρ is the density, M is the molecular weight, n is the number of atoms in the unit cell, and v_m is the mean sound velocity.

The calculated values of longitudinal sound velocity (v_L), transverse sound velocity (v_T), mean sound velocity (v_m) and Debye temperature (θ_D) have been given in Table 4. The higher θ_D suggests the higher thermal conductivity associated with the material. Present study suggests that the value of θ_D is maximum for the spin-polarised TiS₂Cr followed by unpolarized TiS₂Cr and TiS₂.

4. CONCLUSIONS

1. A first principles pseudo potential plane wave method has been utilized to explore the electronic structural and

mechanical properties of unpolarized TiS₂, TiS₂Cr and spin-polarized TiS₂Cr compounds.

2. The lattice constant values of unpolarized TiS₂ and TiS₂Cr compounds are in agreement with the previous theoretical data.

3. The unpolarized TiS₂ and TiS₂Cr compounds display metallic bonding whereas spin-polarized TiS₂Cr shows directional bonding.

4. The unpolarized TiS₂ and TiS₂Cr compounds are associated with ductile behaviour whereas spin-polarized TiS₂Cr compound shows brittle nature.

5. These compounds show anisotropy.

6. The spin-polarized TiS₂Cr shows the maximum value of θ_D followed by unpolarized TiS₂Cr and TiS₂.

ACKNOWLEDGEMENTS

Author is grateful to Ministry of Defence, Government of India for financial support. The author is indebted to Director DMRL Hyderabad for his encouragement. He intends their thanks to Dr. R. Sankarasubramanian for their kind support.

REFERENCES

- Abraham, K. M., & Alamgir, M. (1991). Dimensionally stable MEEP-based polymer electrolytes and solid-state lithium batteries. *Chemistry of Materials*, 3 (2), 339–348.
- Anderson, O. L. (1963). A simplified method for calculating the debye temperature from elastic constants. *Journal of Physics and Chemistry of Solids*, 24(7), 909 – 917.
- Bardhan, K. K., Kirczenow, G., & Irwin, J.C. (1985). High-temperature staging phase diagram of the intercalation compound Ag_xTiS_2 . *Journal of Physics C: Solid State Physics*, 18 (6) L131.
- Baresel, D., Sarholz, W., Scharner, P., & Schmitz, J. (1974). Übergangs-Metallchalkogenide als Sauerstoff-Katalysatoren für Brennstoffzellen. *Berichte der Bunsengesellschaft für physikalische Chemie*, 78(6), 608-611.
- Born, M. (1940). On the stability of crystal lattices. I. *Mathematical Proceedings of the Cambridge Philosophical Society*, 36(2), 160-172.
- Cui, X. Y., Negishi, H., Titov, A. N., Titiv, S. G., Shi, M., & Patthey L. (2006). Evolution of electronic structure on Transition Metal doped Titanium Disulfide by angle-resolved photoemission spectroscopy study. *Condensed Matter Materials Science*, arXiv:1008.1146.
- Fang, C. M., De Groot, R. A., & Haas, C. (1997). Bulk and surface electronic structure of 1 T– TiS_2 and 1 T– TiSe_2 . *Physical Review B*, 56(8), 4455.
- Fedorov, F. I. (1968). Theory of elastic waves in crystals, New York: Plenum, Springer Science & Business Media.
- Goedecker, S. (1997). Fast Radix 2, 3, 4, and 5 Kernels for Fast Fourier Transformations on Computers with Overlapping Multiply – Add Instructions. *SIAM Journal on Scientific Computing*, 18(6), 1605 – 1611.
- Gonze, X., Beuken, J. M., Caracas, R., Detraux, F., Fuchs, M., Rignanese, G. M., Sindic, L., Verstraete, M., Zerah, G., Jollet, F., Torrent, M., Roy, A., Mikami, M., Ghosez, P., Raty, J. Y., & Allan, D. C. (2002). First-principles computation of material properties: the ABINIT software project. *Computational Materials Science*. 25(3), 478 – 492.
- Gonze, X., Rignanese, G. M., Verstraete, M., Beuken, J. M., Pouillon, Y., Caracas, R., Francois, J., Torrent, M., Zerah, G., Mikami, M., Ghosez, P., Veithen, M., Raty, J. Y., Olevano, V., Bruneval, F., Reining, L., Godby, R., Onida, G., Hamann, D. R., & Allan D. C. (2005). A brief introduction to the Abinit software package. *Zeitschrift fuer Kristallographie*. 220(5/6), 558 – 562.
- Gonze, X., Amadon, B., Anglade, P. M., Beuken, J. M., Bottin, F., Boulanger, P., Bruneval, F., Caliste, D., Caracas, R., Cote, M., Deutsch, T., Genovese, L., Ghosez, P., Giantomassi, M., Goedecker, S., Hamann, D. R., Hermet, P., Jollet, F., Jomard, G., Leroux, S., Mancini, M., Mazevet, S., Oliverira, M. J. T., Onida, G., Pouillon, Y., Rangel, T., Rignanese, G. M., Sangalli, D., Shaltaf, R., Torrent, M., Verstraete, M. J., Zerah, G., & Zwanziger, J. W. (2009). ABINIT: First-principles approach to material and nanosystem properties. *Computer Physics Communications*. 180(12), 2582 – 2615.
- Gonze, X. (1996). Towards a potential-based conjugate gradient algorithm for order-N self-consistent total energy calculations. *Physical Review B*, 54(7), 4383.
- Hohenberg, P., & Kohn, W. (1964). Inhomogeneous electron gas. *Phys Rev*, 136(3B), B864.
- Kohn, W. & Sham, L. J. (1965). Self consistent equations including exchange and correlations effects. *Physics Review*, 140(4A), A1133.
- Hill, R. (1952). The elastic behaviour of a crystalline aggregate. *Proceedings of the Physical Society. Section A*, 65(5), 349.
- Inoue, M., Moneta, Y., Neigh, H., & Sasaki, H. (1986). Specific heat measurements of intercalation compounds MxTiS_2 (M= 3d transition metals) using ac calorimetry technique. *Journal of Low Temperature Physics* 63(3-4) 235 – 245.
- Inoue, M., Sadahiro, K., & Negishi, H. (1991). Transport studies on relaxation behaviour in spin-glass phase of itinerant magnetic intercalate Fe_xTiS_2 . *Journal of Magnetism and Magnetic Materials*. 98(1-2), 60 – 64.
- Kim, Y. S., Li, J., Tanaka, I., Koyama, Y., & Adachi, H. (2000). Chemical Bonding around Intercalated Cr and Fe Atoms in TiS_2 . *Materials Transactions. JIM*. 41(8), 1088–1091.
- Kokalj, A. (1999). XCrySDen – a new program for displaying crystalline structures and electron densities. *Journal of Molecular Graphics and Modelling* 17(3-4) 176 – 179; <http://www.xcrysdn.org>
- Negishi, H., Yamada, Y., Yuri, K., & Inoue, M. (1997). Negative magnetoresistance in crystals of the paramagnetic intercalation compound Mn_xTiS_2 . *Physics Review B* 56(17), 11144.
- Matsushita, T., Suga, S., Kimuta, A., Negishi, H., & Inoue M. (1999). Angle-resolved photoemission study of Ni-intercalated 1T – TiS_2 . *Physics Review B* 60(3), 1678.
- Monkhorst, H. J., & Pack, J. D. (1976). Special points for Brillouin-zone integrations. *Physics Review B*, 13(12), 5188.
- Payne, M. C., Teter, M. P., Allan, D. C., Arias, T. A., & Joannopoulos, J. D. (1992). Iterative minimization techniques for ab initio total-energy calculations: Molecular dynamics and conjugate gradients. *Reviews of Modern Physics*, 64(4), 1045.
- Perdew, J.P., Burke, K. & Ernzerhof, M. (1996). Generalized gradient approximation made simple. *Phys Rev Lett*, 77(18), 3685.
- Pettifor, D. G., & Aoki, M. (1991). Bonding and structure of intermetallics: a new bond order potential. *Philosophical Transactions of the Royal Society of London. Series A: Physical and Engineering Sciences*, 334(1635), 439-449.
- Pugh, S. F. (1954). Relations between the elastic moduli and the plastic properties of polycrystalline pure metals. *Philosophical Magazine*, 45, 823.
- Reshak, A. H., Kityk, I. V., & Auluck, S. (2008). Electronic structure and optical properties of 1 T-Ti S 2 and lithium intercalated 1 T-Ti S 2 for lithium batteries. *The Journal of chemical physics*, 129(7), 074706.
- Reuss, A. (1929). Calculation of the bulk modulus of polycrystalline materials. *Ztschr Angew Math Mech*, 9, 49.

- Sharma, S., Nautiyal, T., Singh, G. S., Auluck, S., Blaha, P. & Ambrosch-Draxl, C. (1999). Electronic structure of 1T-TiS₂. *Physical Review B* 59(23), 14833.
- Sharma, Y., Shukla, S., Dwivedi, S. & Sharma, R. (2015). Transport properties and electronic structure of intercalated compounds MTiS₂ (M = Cr, Mn and Fe). *Advanced Materials Letters*. 6(4) 294–300.
- Sun, Z., Li, S., Ahuja, R., & Schneider J. M. (2004). Calculated elastic properties of M₂AlC (M = Ti, V, Cr, Nb and Ta). *Solid State Communications*. 129 (9), 589 – 592.
- Suzuki, N., Yamasaki, Y., & Motizuki, K. J. (1988). Bands and Bonds of Intercalation compounds of Layered Transition-Metal Dichalcogenides. *Journal of Physics Colloques*, 49 (C8) 201 – 202.
- Takase, K., Kubota, Y., Takano, Y., Negishi, H., Sasaki, M., Inoue, M., & Sekizawa K. (2000). Anisotropic magnetic properties of intercalation compound Mn_{1/4}TiS₂. *Physica B: Condensed Matter*. 284 – 288, 1517 –1518.
- Tazake, Y., Saitoh, T., Matsukura, F., Satoh, T., Mayadai, T., & Hoshi K. (1988). Properties of Ising Magnetic System Fe_xTiS₂. *Journal of Physics Colloques*. 49(C8)1507 – 1508.
- Tonti, D., Pettenkofer, C., & Jaegermann W. (2004). Origin of the Electrochemical Potential in Intercalation Electrodes: Experimental Estimation of the Electronic and Ionic Contributions for Na Intercalated into TiS₂. *Journal of Physical Chemistry B* 108 (41) 16093– 16099.
- Ueda, Y., Negishi, H., Koyana, M., Inoue, M., Soda, K., Sakamoto, H., & Suga S. (1986). Resonant photoemission studies of 3d transition metal intercalates of TiS₂. *Solid State Communications*, 57(10), 839 – 842.
- Voigt, W. (1928). *Lehrbuch der Kristallphysik*, Teubner, Leipzig.
- Whittingham, M. S. (1987). Chemistry of intercalation compounds: Metal guest in Chalcogenide hosts. *Progress in Solid State Chemistry*. 12(1) 41–99.
- Yamasaki, T., Suzuki, N., & Motizuki K. (1987). Electronic structure of intercalated transition-metal dichalcogenides: M_xTiS₂ (M = Fe, Cr). *Journal of Physics C: Solid State Physics* 20 (3) 395.
- Yan-Bin, Q., Guo-Hua, Z., Li, D., Jiang-Long, W., Xiao-Ying, Q., & Zhi, Z. (2007). Strongly correlated effect in TiS₂. *Chinese Physics Letters*, 24(4) 1050.